August 27-31, 2023
FLORENCE - ITALY
ICWE 16
16th International Conference on Wind Engineering

Accurate representation of cyclists' body positions in CFD simulations via linear blend skinning: a validation study

B. Van Gael [1], T. van Druenen[1]

[1] *Building Physics and Services, Department of the Built Environment, Eindhoven University of Technology, 5600, MB Eindhoven, the Netherlands, b.j.c.van.gael@tue.nl*

SUMMARY
In this study, computational fluid dynamics (CFD) simulations were applied together with the linear blend skinning (LBS) method to investigate the effects of body position on aerodynamic drag in cycling. A 3D scanner was used to create a virtual geometry of an elite male cyclist, which was then deformed using LBS to represent varying body positions. To validate the morphological accuracy of the LBS method, the results of CFD simulations were compared to experimental data from wind tunnel (WT) tests for three different body positions. Similar trends were obtained for the CFD simulations and WT tests. Compared to the reference position, the drag of the cyclists was reduced by 1.8% (WT) and 2.3% (CFD) for position 2 and by 7.6% (WT) and 6.3% (CFD) for position 3. These results show that small variations in position can have a significant impact on the aerodynamic drag, highlighting the importance of proper positioning of the cyclist's body for optimizing cycling performance.

Computational Fluid Dynamics (CFD), Linear blend skinning (LBS), Sports Aerodynamics, Wind tunnel testing, Aerodynamic drag

1. INTRODUCTION

Reducing aerodynamic drag is crucial for optimizing cycling performance, especially at high speeds. At 50 km/h, aerodynamic resistance is about 90% of the total resistance of a solo cyclist on a flat surface (Grappe et al., 1997; Kyle & Burke, 1984). It was estimated that 60-70% of the total aerodynamic drag is caused by their bodies (Gross et al., 1983). As a result, minimizing body aerodynamic drag is a critical objective for elite cyclists.

Traditionally, wind tunnel (WT) measurements have been executed to assess and reduce drag. In method, elite cyclists typically spend a large amount of time in the WT, iteratively adjusting their position to incrementally minimize drag. In general, this approach can be costly and time-consuming for athletes. In addition, it can also be challenging for them to maintain a fixed position, which can introduce additional uncertainty to the results, limiting the accuracy.

The use of computational fluid dynamics (CFD) simulations offers a valuable alternative to traditional WT testing for analyzing cycling aerodynamics. By generating detailed data on the whole flow field, CFD enables a comprehensive analysis of the local airflow around the athlete. This approach has the potential to become more efficient and cost-effective for optimizing cycling performance due to the increasing computational power available. Previous research has used Computer-Aided Design to represent the human body by simplifying the geometries of the torso, arms, and legs (i.e. Griffith et al., 2014). While this approach allows for easy geometry adjustment,

it also results in an oversimplification of the body's true shape, reducing the ability to accurately identify individual areas of improvement or *'marginal gains'*. Other research has utilized high-quality structured-light 3D scanning to generate more realistic and accurate computational geometries of the cyclist (i.e. Blocken et al., 2018). However, the unstructured and static point-cloud representation generated by the scanning process requires a significant amount of post-processing time to create a clean geometry for usage in CFD simulations. This may be a limiting factor in the number of body positions that can be analyzed using this method.

2. LINEAR BLEND SKINNING

Linear blend skinning (LBS) is a method for generating multiple realistic body positions from a single 3D scan, eliminating the need to scan each position separately (Mohr & Gleicher, 2003). The method consists of linking the mesh vertices of the body geometry to an underlying skeletal structure. The skeletal structure is composed of n bones, and to specify the relation between bone i and the location $\overrightarrow{r_k}$ of vertex *k*, a normalized blend weight $w_{i,k,norm}$ is assigned to vertex *k*. This weight determines the influence of the bone transformation on the position of the vertex, as described by Equation (1), where $\boldsymbol{T_i}$ represents the transformation matrix of bone *i*.

$$\overrightarrow{r_k} = \sum_{i=1}^{n}(w_{i,k,norm} \times \boldsymbol{T_i} \times \overrightarrow{r_{k,0}}) \quad (1)$$

$$w_{i,k,norm} = \frac{w_{i,k}}{\sum_{i=1}^{n} w_{i,k}} \quad (2)$$

$$w_{i,k} = 1 - \frac{d_{i,k}}{r_i} \text{ for } d_{i,k} < r_i \text{ and } w_{i,k} = 0 \text{ for } d_{i,k} \geq r_i \quad (3)$$

The bone structure was constructed manually and normalized blend weights were assigned to the mesh vertices using a weight function (Blender Foundation, 2021), which assigns weights to the vertices based on their proximity to the bones, as described by Equations (2) and (3) where $d_{i,k}$ is the distance between bone *i* and vertex *k*, and r_i describes the radius of influence for bone *i*.

3. WIND TUNNEL MEASUREMENTS

WT measurements were conducted at Eindhoven University of Technology. The test section had dimensions of 3 × 2 m². The cyclist was mounted on a platform with a drag force sensor and a customized support system. The drag force on the platform and support system was subtracted from the measured drag of the entire system to isolate the aerodynamic drag of the cyclist from the support system. Air temperature, atmospheric pressure, humidity and free wind speed were recorded during the measurements. Wind speed was 15 m/s and turbulence intensity was about 0.5% at the position of the cyclist.

4. CFD SIMULATIONS

According to best practice guidelines (Tominaga et al., 2008), full-scale CFD simulations were carried out in a computational domain with dimensions L × W × H = 46.7 × 17.5 × 18 m³. A single 3D scan was used to obtain the computational geometry of the cyclist. The bicycle was excluded from the computational geometry to save on computational resources. It was assumed that the bicycle would not affect the relative aerodynamic performance of the different body positions. The cyclist's geometry was adjusted using LBS to match its position during a set of three WT tests. This was done by comparing the side view of the computational geometry with contour images acquired during the WT tests (Fig. 1). The joint angles of the three body positions, as defined in Fig. 2a, are provided in Table 1a.

Taking into account guidelines for grid generation in CFD (Franke et al., 2007; Tominaga et al., 2008; Tucker & Mosquera, 2001), poly-hexcore grids (Fig. 2b) were generated which contained approximately 12 million cells each. The 3D RANS CFD simulations were performed with the commercial CFD code Ansys Fluent 2021 R1 (ANSYS Inc, 2021), using the Transition SST turbulence model to approximate the Navier-Stokes equations. The pressure-velocity coupling was treated as coupled, and gradients were calculated using the Green-Gauss Cell-Based method. The spatial discretization was carried out using second-order schemes. The inlet velocity was set to 15 m/s, with a turbulence intensity of 0.5%. The pseudo time step was 0.01 s and results were sampled over 5,000 iterations to obtain a constant moving average of the sampled drag force. The roughness height on the body surface was set to 0.1 mm and the surface on the helmet was considered smooth.

5. RESULTS

Table 1 shows the results of the WT tests and CFD simulations with column b presenting the results as a percentage of the drag of body position 1 obtained in the WT test. Due to the absence of the bicycle in the computational geometry, drag area values ACd [m²] were about 27% lower for the CFD simulations compared to the WT tests. Column c presents the results as a percentage difference of the drag of body position 1 for both WT and CFD. Here, similar trends were observed. Compared to body position 1, relatively small drag reductions of 1.8% (WT) and 2.3% (CFD) were calculated for body position 2, while larger drag reductions of 7.6% (WT) and 6.3% (CFD) were obtained for body position 3.

Table 1. Joint angles and drag area values for three body positions

	a. Joint angle [°]							b. $\frac{ACd_i}{ACd_{ref}}$ [%]		c. Difference [%]	
Body position	**1 Forearm**	**2 Elbow**	**3 Shoulder**	**4 Torso**	**5 Hip**	**6 Knee**	**7 Foot**	**WT**	**CFD**	**WT**	**CFD**
1	6.3	89.7	80.3	15.8	55.2	105.4	12.8	100 (ref)	73.7	-	-
2	14.2	79.8	78.8	15.3	53.1	103.2	21.0	98.2	71.4	-1.8%	-2.3%
3	17.6	73.4	78.3	12.7	51.7	106.0	12.8	92.4	67.4	-7.6%	-6.3%

6. DISCUSSION

The use of LBS for the adjustment of body positions resulted in similar drag reductions obtained in the CFD simulations compared to those obtained during WT testing. Discrepancies between CFD and WT results may be due to the absence of the bicycle, simplifications in surface roughness modeling, and deviations in body position due to manual alignment. To fully understand the implications of using LBS for CFD simulations, it is essential to run simulations for a wider range of body positions to evaluate its full potential and limitations. Additional research will be required to test variants for LBS to determine the most effective approach for modifying virtual body morphologies in order to improve cycling aerodynamics using CFD.

Figure 1. Geometric comparison using side contours of virtual geometry (red) and geometry during WT tests (black)

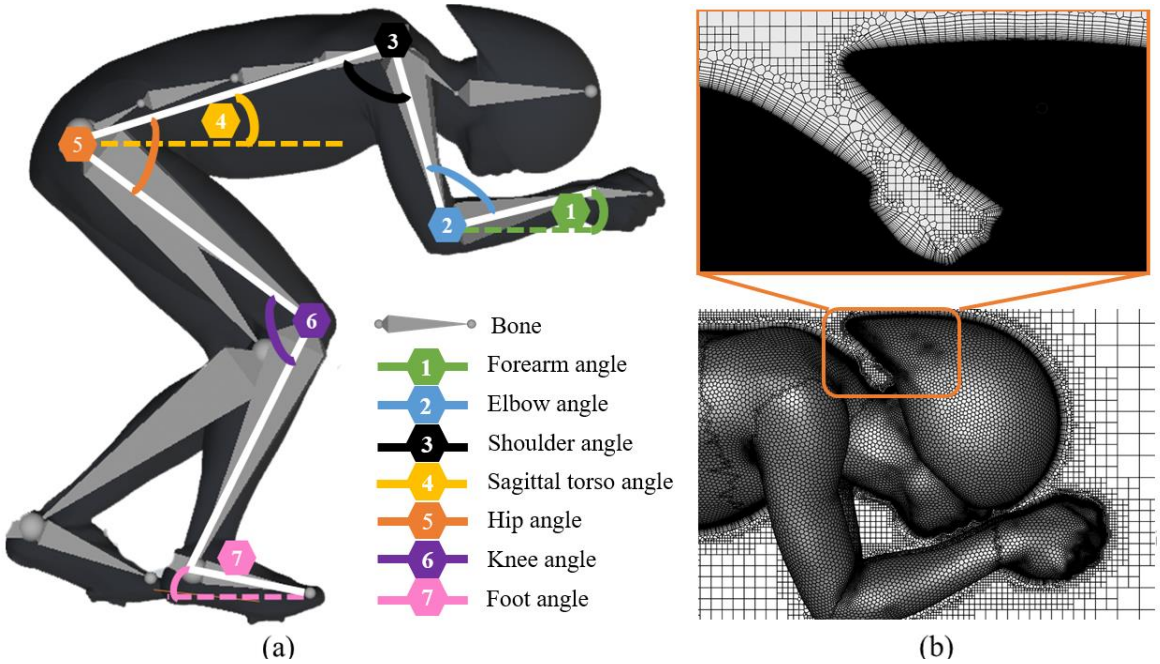

Figure 2a. Visualization of bones and joint angles in the virtual geometry **Figure 2b.** Computational grid

ACKNOWLEDGEMENTS

We would like to extend our sincere gratitude to Ansys and Team Jumbo Visma for their support in this research project. We are deeply grateful for their contributions and look forward to continuing our collaboration in the future.

REFERENCES

ANSYS Inc. (2021). *ANSYS, Fluent, January 2021, Release 2021 R1, Tutorial Guide*.

Blender Foundation. (2021). *Blender* (2.92.0). Blender Foundation.

Blocken, B., van Druenen, T., Toparlar, Y., & Andrianne, T. (2018). Aerodynamic analysis of different cyclist hill descent positions. *Journal of Wind Engineering and Industrial Aerodynamics*, *181*, 27–45.

Franke, J., Hellsten, A., Schlünzen, K. H., & Carissimo, B. (2007). Best practice guideline for the CFD simulation of flows in the urban environment-a summary. *11th Conference on Harmonisation within Atmospheric Dispersion Modelling for Regulatory Purposes, Cambridge, UK, July 2007*.

Grappe, F., Candau, R., Belli, A., & Rouillon, J. D. (1997). Aerodynamic drag in field cycling with special reference to the Obree's position. *Ergonomics*, *40*(12), 1299–1311.

Griffith, M. D., Crouch, T., Thompson, M. C., Burton, D., Sheridan, J., & Brown, N. A. T. (2014). Computational fluid dynamics study of the effect of leg position on cyclist aerodynamic drag. *Journal of Fluids Engineering*, *136*(10).

Gross, A. C., Kyle, C. R., & Malewicki, D. J. (1983). The aerodynamics of human-powered land vehicles. *Scientific American*, *249*(6), 142–153.

Kyle, C. R., & Burke, E. (1984). Improving the racing bicycle. *Mechanical Engineering*, *106*(9), 34–45.

Mohr, A., & Gleicher, M. (2003). Building efficient, accurate character skins from examples. *ACM Transactions on Graphics (TOG)*, *22*(3), 562–568.

Tominaga, Y., Mochida, A., Yoshie, R., Kataoka, H., Nozu, T., Yoshikawa, M., & Shirasawa, T. (2008). AIJ guidelines for practical applications of CFD to pedestrian wind environment around buildings. *Journal of Wind Engineering and Industrial Aerodynamics*, *96*(10–11), 1749–1761.

Tucker, P. G., & Mosquera, A. (2001). *NAFEMS introduction to grid & mesh generation for CFD* (Vol. 79). NAFEMS.